



Original Article

Estimating the effect of climate change on water resources: Integrated use of climate and hydrological models in the Werii watershed of the Tekeze river basin, Northern Ethiopia

Gebremedhin Gebremeskel^{a,*} Asfaw Kebede^b^a Irrigation and Water Resources, Tigray Agricultural Research Institute, Mekelle, Ethiopia^b Hydraulics and Water Resources Engineering, Institute of Technology, Haramaya University, Dire Dawa, Ethiopia

ARTICLE INFO

Article history:

Received 9 January 2017

Accepted 27 October 2017

Available online 17 July 2018

Keywords:

Climate change

SDSM

Water resources

Werii watershed

WetSpa

ABSTRACT

This paper presents the effect of climate change on water resources in the Werii watershed (1797 km^2) using climate (SDSM) and hydrological (WetSpa) models. A fully distributed model (WetSpa) was used to simulate the water resources of the base (2004–2010) and future (2015–2050) periods. The digital elevation model (DEM), land-use, soil and hydro-meteorological features of the Werii watershed were used as inputs to the WetSpa model. Likewise, the statistical downscaling model (SDSM) was used to downscale climate projections from the regional climate model (REMO) which in turn would be used as input for the WetSpa model for future water resources simulation based on A1B and B1 special report for emission scenarios (SRES). Simulations of the SDSM and WetSpa models showed that rainfall will be increased by 24% under A1B and 25.3% under B1. The minimum and maximum temperatures will also increment by 0.17 and 0.09 °C, respectively, under A1B and by 0.16 and 0.07 °C under B1, respectively. Similarly, for A1B and B1, positive changes are likely to occur for baseflow by 14% and 8%, respectively, for recharge by 5% and 2%, respectively, and for evapotranspiration by 15% and 18%, respectively. However, the surface runoff would decrease by 13% and 14%, respectively, under similar trends from the base period. This implies that a positive change is likely in the future water balance components of the watershed with the exception of runoff. As a result, increased exploitation of the water resources comparable to the resources increment is advised. However, optimized water resources allocation is worthwhile, providing it is in a sustainable way.

Copyright © 2018, Kasetart University. Production and hosting by Elsevier B.V. This is an open access article under the CC BY-NC-ND license (<http://creativecommons.org/licenses/by-nc-nd/4.0/>).

Introduction

Water is a fundamental entity for living things as there is no living creature which does not depend on water, directly or indirectly (Kumar, 2012). Specifically, Alcamo et al. (1997) indicated that water plays an essential role in the existence of human beings, which is why people become more vulnerable when a shortage of water exists. Even if adequate water resources are available globally, its spatial and temporal distribution remain uneven (Raghunath, 2006). This is now more pronounced due to the higher rate of population growth, enhanced living standards, extreme water pollution and global climate change effects (Intergovernmental Panel on Climate Change, 2013).

Ethiopia is considered as the water tower of Africa (Makombe et al., 2007), due to its abundant water resources on the surface and subsurface despite its erratic rainfall. It has 12 river basins with a total annual water resource estimated at 111 billion m^3 of which 75.5 billion m^3 is in the Nile basin (Yazew, 2005; Gebremeskel and Kebede, 2017). In addition, the country releases an annual runoff volume of 122 billion m^3 of water to neighboring countries (Awulachew et al., 2007). The Abay, Baro-Akobo, Omo-Gibe and Tekeze river basins are considered as the main runoff contributors. Knowledge available on groundwater resources of Ethiopia is scanty and lacks consensus. It needs a detailed study so that accurate information can be obtained. It is reported that groundwater potential is less than the water found on the surface (Awulachew et al., 2007). This indicates that there is an ample amount of water with regards to geographical positions.

Studies have shown that the threat of climate change impacts on the water resources of Ethiopia. Melesse (2011) and Soliman et al.

* Corresponding author.

E-mail address: medkel17@gmail.com (G. Gebremeskel).

(2009) indicated that climate change in the upper Blue Nile basin of Ethiopia would occur and would shift and reshape the annual and seasonal climate patterns and variation in rainfall, reduce reservoir yield and cause erratic rainfall. Similarly, Kebede et al. (2013) indicated that an increasing trend of annual maximum temperature and annual future rainfall with seasonal variations was observed in the Baro-Akobo Basin. Currently, variations in frequency, distribution, and intensity of rainfall are the common phenomenon in the country. Since, the country's economy is mainly dependent on rain-fed agriculture (Makombe et al., 2007), the people are exposed to food insecurity if the climate change impact on the existing water resource is not properly addressed. The Tigray region, where the Werii watershed is located, is similarly affected by climate change, which is indicated through recurrent droughts as a result of the erratic and general shortage of rainfall (Araya and Stroosnijder, 2011; Gebrehiwot and van der Veen, 2013; Hadgu et al., 2013, 2015). This paper presents an application of the WetSpa model for the base period and for future water resources simulation. It is a physically based, fully distributed hydrological model (Liu and De Smedt, 2004) which has been widely applied in different parts of the world, including in Ethiopia, in the Geba catchment (Beyene et al., 2011) and in Uganda, in the Upper Ssezibwa catchment (Nyenje and Batelaan, 2009). The SDSM model was also used to downscale the regional climate information from REMO datasets. This model has been applied in different parts worldwide (Paeth et al., 2005; Kebede et al., 2013). The current study focused on estimating the effect of climate change in the future (2015–2050) water balance components in the Werii watershed, in the Tekeze river basin, through the integrated use of climate (SDSM) and hydrological (WetSpa) models. Therefore, in the watershed an estimation of the base period water resources and simulation of future hydrological changes due to the effect of climate change was assessed based on emission scenarios.

Materials and methods

Study area description

This study was conducted in the Tekeze river basin, Werii watershed (1797 km^2), Northern Ethiopia (Fig. 1 & Table 1). The watershed is surrounded by the Geba watershed in the southeast, the Mereb River basin in the north and the middle Tekeze River basin in the west. It extends from $13.843^\circ \text{ to } 14.27^\circ \text{N}$ and $39.467^\circ \text{ to } 39.016^\circ \text{E}$. The gauging station (13.843°N , 39.016°E) is located at the outlet of the Werii watershed on the road between the towns of Abiyadi and Adwa.

The watershed is highly vulnerable to soil erosion due to its steep landscape characteristics. The mean elevation and slope of the watershed are 1951 m above sea level and 19%, respectively (Gebremeskel and Kebede, 2017). Rainfall distribution is uni-modal and mostly erratic with distinct dry and wet seasons. The agricultural system is mainly mixed agriculture. The agricultural basis is Gesho (*Rhamnus prinoides*) farming and highland crops in the upstream and agroforestry practices downstream of the watershed. Silt-clay loam, sandy loam, and silty loam are the dominant soil types found in the watershed (Food and Agriculture Organization of the United Nations [FAO], 1998). Similarly, land use types such as crop-land, shrub, forest and bare land are mainly found in the Werii watershed. Paleozoic sedimentary rock known as Edaga-Arbi Tillites is also widely distributed in the watershed (Tesfamichael et al., 2013).

Application of WetSpa model

The WetSpa model (Wang et al., 1997; Liu and De Smedt, 2004) was used for the base period and future water resources

components estimation. WetSpa stands for Water and Energy Transfer between Soil, Plants and Atmosphere on a regional or basin level (Wang et al., 1997). This hydrological model is GIS based and it uses the Arc-View GIS (ESRI; Redlands, Ca, USA) environment through a WetSpa extension. It simulates the hydrological processes of precipitation, interception, surface runoff, infiltration, evapotranspiration, percolation, interflow and groundwater flow (Liu and De Smedt, 2004). The model conceptualizes a basin hydrological system, based on physical and empirical relationships (Fig. 2). Data inputs to the model were digital maps prepared with the help of GIS packages and parameter files from spreadsheet tables with their specific extensions (Liu and De Smedt, 2004).

The input parameter files were the daily records of hydro-meteorological parameters such as precipitation, potential evapotranspiration, temperature, and discharge. The land use, soil type, and topography were the base maps from which the gridded model parameter files and maps were derived and combined with attribute files. The parameter tables were time series data which contained land-use type described by rooting depth, leaf area index and vegetation height. It also contained soil parameters for each textural class such as field capacity, wilting point, and permeability.

In this study, the water balance components were investigated using the WetSpa model based on groundwater balance Eq. (1) (Liu and De Smedt, 2004) expressed as Eq. (1):

$$SG_s(t) = SG_s(t-1) + \frac{\sum_{i=1}^{N_s} [RG_i(t)A_i]}{A_s} - EG_s(t) - \frac{QG_s(t)\Delta t}{1000A_s} \quad (1)$$

where; $SG_s(t)$ and $SG_s(t-1)$ are groundwater storage of the watershed at time steps t and $t-1$ (in millimeters), N_s is the number of cells in the watershed, A_i is the cell area (in square meters), A_s is the watershed area (in square meters), $RG_i(t)$ groundwater recharge (in millimeters), $EG_s(t)$ is the average evapotranspiration from groundwater storage of the watershed (in millimeters), and $QG_s(t)$ is the groundwater discharge (cubic meters per second) and s and i represent the watershed and number of cell with corresponding time steps, respectively.

At the root zone level, 2009 At the root zone level, the water balance was used to control runoff, interflow and groundwater recharge for each grid cell (Nyenje and Batelaan, 2009) calculated using Eq. (2):

$$D \frac{\Delta \theta}{\Delta t} = P - I - S - E - F - R \quad (2)$$

where D is the root zone depth (L); $\Delta \theta$ is the change in soil moisture content ($L^3 L^{-3}$); Δt is the time interval (T); P is the precipitation (LT^{-1}); I is the initial abstraction (interception and depression losses) in (LT^{-1}); S is the surface runoff (LT^{-1}); E is the actual evapotranspiration (LT^{-1}); F is the interflow (LT^{-1}) and R is the percolation out of the root zone (LT^{-1}).

The percolation from the root zone recharges the groundwater storage, which then contributes to groundwater discharge forming the base flow (Liu and De Smedt, 2004). The recharge was estimated based on the relationship between hydraulic conductivity and effective saturation (Brooks and Corey, 1966) as shown in Eq. (3):

$$R = K_s \left(\frac{\theta - \theta_r}{\theta_r - \theta_s} \right)^{(2+3B)/B} \quad (3)$$

where R is the recharge or percolation (in millimeters per hour), K_s is the saturated soil hydraulic conductivity (in millimeters per hour), θ is soil moisture content (in cubic meters per cubic meter), θ_r is the residual moisture content (in cubic meters per cubic

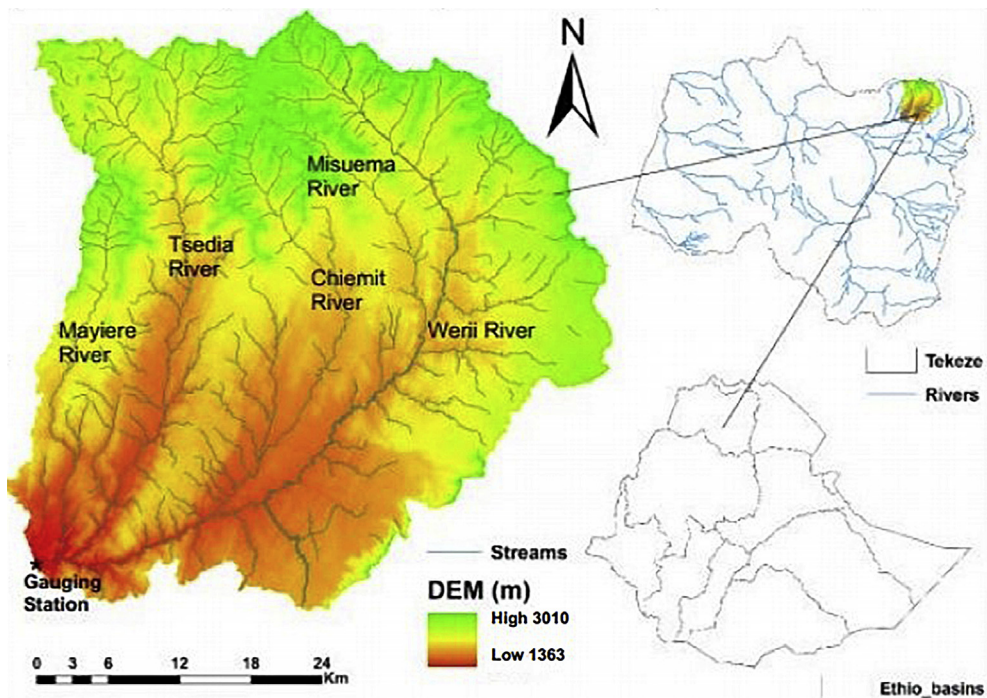


Fig. 1. Geographical location map of Werii watershed in Tekeze river basin and drainage networks, major tributaries and gauging station location.

meter), θ_s , soil porosity (in cubic meters per cubic meter) and B is the pore size distribution index (–).

Moreover, in the WetSpa model, the general water balance system is expressed using Eq. (4):

$$P = RT + ET + \Delta SS + \Delta SG \quad (4)$$

where P is the precipitation in the watershed over the simulation period (in millimeters), RT and ET are total runoff and total evapotranspiration (in millimeters), ΔSS is the change in soil moisture storage for the watershed between the start and the end of the simulation period (in millimeters), and ΔSG is the change in groundwater storage of the watershed (in millimeters).

WetSpa model input parameters and data sources

The WetSpa model applies non-spatial hydro-meteorological datasets and spatial biophysical features of the watershed. Hence, the digital elevation model (DEM), spatial soil type and land use maps of the watershed were used as inputs for the model. For the

elevation map, a high resolution ASTER (advanced spaceborne thermal emission and reflection radiometer) $30 \text{ m} \times 30 \text{ m}$ DEM was used (<http://aster.usgs.gov>). Soil type and land use maps were taken from FAO archives (<http://www.africover.org/index.htm>). A slope map of the watershed was derived from the topographic maps with the help of Arc GIS.

The discharge data were available from the recording station at the outlet of the Werii watershed. Rainfall data were taken from four meteorological stations (Abyiadi, Adwa, Hawzen and Adigart) in and around the watershed. Potential evapotranspiration (PET) was estimated using Hargreaves equation (Allen et al., 1998). All the data were provided on a daily basis for the model. The average monthly rainfall, evapotranspiration, and discharge are summarized in Fig. 3 which illustrates the available measured data that were used for the calibration (2004–2007) and validation (2008–2010) periods of the WetSpa model.

The general physiographic features of the watershed, which incorporated watershed boundary, major contributing river networks and the gauging station at the outlet are presented in Fig. 1. Moreover, the watershed physical parameters with their

Table 1
General watershed characteristics and data record periods used in the WetSpa model.

Parameter	Magnitudes/scale/time period	Sources
Area	1797 km^2	Arc GIS delineation
Perimeter	299 km	Arc GIS delineation
Lowest elevation	1363 m above sea level	Arc GIS delineation
Mean watershed elevation	1951 m above sea level	Calculation
Highest elevation	3010 m above sea level	Arc GIS delineation
Outlet (gauging station)	13.843°N and 39.016°E	Measurement
DEM	$30 \text{ m} \times 30 \text{ m}$	ASTER
Soil map	1:5,000,000	FAO
Land use map	300 m (2005)	FAO
Discharge (m^3/s)	2004–2010	MoWIE
Rainfall (mm/d)	2004–2010	NMA
Potential evapotranspiration (mm/d)	2004–2010	Estimation

MoWIE = Ethiopian Ministry of Water Resources, Irrigation and Energy, NMA = Ethiopian National Meteorological Agency.

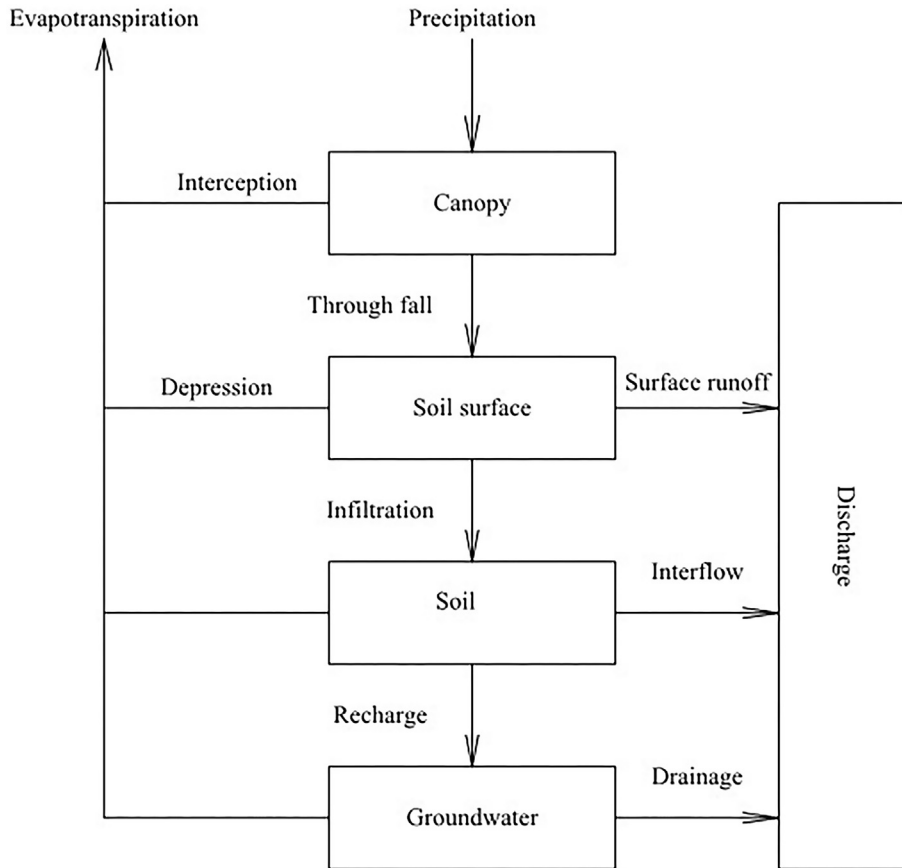


Fig. 2. Structure of WetSpa hydrological model at a pixel cell level (Liu and De Smedt, 2004).

corresponding values and data sources are briefly listed in Table 1. The meteorological data ranges for each of the stations and their measurement and sources are also presented in Tables 1 and 2.

The Thiessen polygon method was used to estimate the area-based rainfall of the catchment. The geographical coordinates of the station and the delineated watershed boundary were used in the GIS to capture the grids for daily rainfall and potential evapotranspiration. Base period and future changes in the Werrii watershed water resources were simulated after having the WetSpa model calibrated and validated using the input data.

WetSpa model evaluation criteria

Statistical measures providing quantitative estimates for the goodness of fit between the observed and predicted values were

used as indicators of the extent to which model predictions matched observation (Liu and De Smedt, 2004). The model performance was evaluated for both the calibration and validation period. The lists of the main model performance evaluation criteria embedded in WetSpa by the model developers (Wang et al., 1997; Liu and De Smedt, 2004) are given below and were used in this study.

Model bias

This is the relative mean difference between the predicted and observed stream flows for a sufficiently large simulation sample, reflecting the ability to reproduce water balance. It is an important criterion for comparing whether a model is working well or not by measuring the presence of under or over prediction. Model bias is given by Eq. (5):

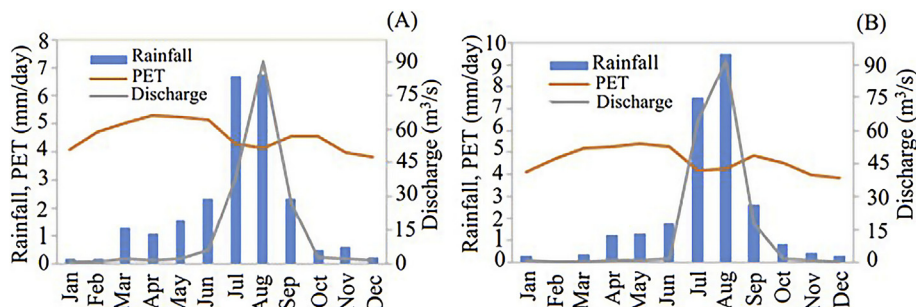


Fig. 3. Measured mean monthly rainfall, potential evapotranspiration (PET) and discharge data of the watershed for WetSpa model calibration and validation periods.

Table 2

Rainfall, daily minimum and maximum temperatures data record periods used by the SDSM model in the Werri watershed.

Meteorological station	Altitude (m above sea level)	Latitude (degrees)	Longitude (degrees)	Data ranges (year range)	Years with missed data
Abyadi	1,829	13.53	39.01	1971–2010	5
Adwa	1,911	14.16	38.90	1971–2010	5
Hawzen	2,242	13.98	39.43	1971–2010	5
Adigrat	2,497	14.26	39.45	1971–2010	5

$$MB = \frac{\sum_{i=1}^N (Qs_i - Qo_i)}{\sum_{i=1}^N Qo_i} \quad (5)$$

where MB is the model bias, Qs_i and Qo_i are the simulated and observed stream flows at time step i (in cubic meters per second) and N is the number of time steps over the simulation period.

A lower MB value indicates a better fit, and the value 0.0 represents the perfect simulation of observed flow volume. Model bias values tend to vary more during dry periods than during wet periods for streamflow (Gupta et al., 1999). It is useful to consider the behavior of these criteria when using split-sample data for calibration and validation. Model simulation values were accepted if the MB values were in between –0.25 and 0.25 for stream flows (Moriasi et al., 2007).

Model confidence

Model confidence expressed using the coefficient of determination is one of the important criteria in the assessment of continuous model simulation. It is calculated as the sum of the squares of the deviations of the simulated and observed discharges from the average observed discharge (Eq. (6)).

$$R^2 = 1 - \frac{\sum_{i=1}^N (Qs_i - \bar{Qo})^2}{\sum_{i=1}^N (Qo_i - \bar{Qo})^2} \quad (6)$$

where R^2 is the model determination coefficient and \bar{Qo} is the mean observed streamflow over the simulation period.

R^2 value varies between 0 and 1, with a value close to 1 indicating a higher level of model confidence with less error of variance and model simulation is acceptable if the R^2 value is greater than 0.5 (Santhi et al., 2001). R^2 is very sensitive to outliers and less sensitive to additive and proportional difference values between simulated and observed data (Legates and McCabe, 1999). However, R^2 has been widely used for model evaluation.

Nash-Sutcliffe efficiency

Nash and Sutcliffe (1970) developed model evaluation criteria into the Nash-Sutcliffe coefficient (NSE), which is used to describe how well the discharge is simulated by the model. This efficiency criterion is commonly used for model evaluation (Eq. (7)).

$$NSE = 1 - \frac{\sum_{i=1}^N (Qs_i - Qo_i)^2}{\sum_{i=1}^N (Qo_i - \bar{Qo})^2} \quad (7)$$

where the NSE value can range from a negative value to 1, with 1 indicating a perfect fit between the simulated and observed hydrographs. NSE is used to calibrate highly variable flow regimes characterized by extreme high flows and extremely low flow events (Moriasi et al., 2007). Hence, NSE was found to be the best objective function for reflecting the overall fit of a hydrograph. Model simulation can be judged as satisfactory if NSE is greater than 0.50 (Moriasi et al., 2007).

Statistical downscaling of climate change scenarios

The statistical downscaling model (SDSM) (Wilby et al., 2004; Wilby and Dowson, 2007) was used to downscale the regional climate model (REMO) (<http://www.remo-rcm.de>) for climate change projections in the Werri watershed. The REMO is a hydrostatic regional climate dataset model developed at the Max Planck Institute on the basis of the former Europamodell of the German Weather Service (Jacob, 2001). The SDSM model was calibrated to create the best fit relationships among the SDSM parameters, which relates REMO predictor variables to local-scale meteorological data series (predictands). The relationships were then used to downscale future climate changes using REMO predictor variables for A1B and B1 SRES (Special Report for Emission Scenarios) emission scenarios (Haile and Kassa, 2015). The SDSM model calibration process was implemented based on an average of 20 ensembles used for the analysis of the climate variables. Details on how to use these ensembles for the Werri watershed are in Haile and Kassa (2015). Even if there are newly emerged representative pathway scenarios (Moss et al., 2010), the emission scenarios are still valid to use for climate predictions. Hence, the A1B and B1 emission scenarios were selected as the watershed is believed to have a balanced (A1B) and sustainable (B1) economic development with corresponding emission and socioeconomic changes in the future. Hence, the A1B and B1 emission scenarios were used as an experimental treatment for which the climate change projections were estimated. The predictands considered were the locally observed daily minimum temperatures (T_{min}), maximum temperatures (T_{max}) and rainfall data series, for each meteorological station (Adigrat, Hawzen, Adwa and Abyadi) in the watershed. These meteorological stations were selected based on data accessibility and proximity to the watershed. The location and data ranges of the selected meteorological stations are given in Table 2.

The observed daily rainfall and temperature data in the period 1971–1985 were used for SDSM model calibration. Likewise, the daily meteorological data recorded during 1991–2010 were also used for model validation. The data period 1986–1990 was not considered as there were no recorded meteorological data from the stations.

The SDSM model calibration process was evaluated using the standard deviation (SD) and mean absolute error (MAE), where the latter is a quantity used to measure how close simulated forecasts are from the observed data (Willmott and Kenji, 2005). The SDSM model increases its perfection when the MAE approaches zero. The MAE is calculated using Eq. (8):

$$MAE = \frac{1}{n} \sum_{i=1}^n |f_i - y_i| \quad (8)$$

where f_i is the predicted value and y_i is the observed value.

As the potential evapotranspiration (PET) is a vital input value for the WetSpa model, it was calculated using the Hargreaves equation as given in Eq. (9) (Allen et al., 1998). The PET is calculated as a function of temperature with some constant values for the Werri watershed. As a result, the observed and downscaled daily minimum and maximum temperature were used to estimate the

base period and future PET time series data, respectively. The calculated daily PET values were used as input for the WetSpa model to simulate the water balance components of the watershed.

$$\text{PET} = 0.0023(\text{T}_{\text{mean}} + 17.8)(\text{T}_{\text{max}} - \text{T}_{\text{min}})^{0.5} \text{R}_a \quad (9)$$

where PET is the potential evapotranspiration (in millimeters per day); T_{mean} , T_{max} and T_{min} are average, maximum and minimum temperatures (in degrees Celsius), respectively, and R_a is extraterrestrial radiation (in millimeters per day).

The downscaled average daily time series data of rainfall and the calculated PET, for all the stations considered in the watershed, were used as input for the validated WetSpa model to simulate the hydrological water balance components in the future.

Results and discussion

WetSpa model simulation process, physical parameter derivations, and lookup tables

Gridded model parameter maps were derived from the topography, land use and soil maps of the watershed together with an attribute lookup table prepared in dbf format. Physiographic features of the watershed such as surface slope, hydraulic radius, flow direction, flow accumulation, stream network and order as well as sub-catchments were delineated from the DEM. As a result, 96 sub watersheds having an average area of 18.7 km^2 were simulated and the simulated time of concentration was estimated 58 h with 23 h mean travel time (Table 3).

From the soil map of the watershed, the soil hydraulic conductivity, pore size distribution index, plant wilting point porosity, field capacity and residual moisture for each grid cell were derived. Similarly, the Manning's roughness coefficient, interception storage capacity and root depth parameters were derived from the

land use map. In addition, a combination of elevation, soil and land use grids were used to provide grids of the potential runoff coefficient and depression storage capacity of the watershed by means of attribute lookup tables. To compute the instantaneous unit hydrograph flow from each grid cell to the watershed outlet; travel time to the basin outlet, grids of flow velocity and standard deviation were generated in the final time step. During the derivations of the parameters and coefficients related to the WetSpa model, threshold and constant values were generated in the simulation process. Parameter values that were taken as a threshold value and derived from other parameters and watershed constants are listed in Table 3.

The cell area, cell size and the number of rows and columns of the watershed had to be similar for all the base maps of topography, land use and soil type. This helped the WetSpa model to perform the simulations properly. Accordingly, the watershed base maps were made using a 100 m grid cell size with an average of 510 and 718 row and columns, respectively.

WetSpa model calibration and validation

Calibration processes comprise deriving parameter values and characteristic effects, equation constants and weighting factors that serve to define the model for the study watershed (Liu and De Smedt, 2004). The most useful list of the calibration parameters and corresponding measurement units of the model are given in Table 4.

According to Liu and De Smedt (2004), the interflow scaling factor (K_i) is a parameter for reflecting the organic matter in plants root zone associated with soil hydraulic conductivity. The groundwater flow recession coefficient (K_g) is a global parameter for reflecting a catchment's groundwater recession regime and the relative soil moisture parameter (K_{ss}) is related to the field capacity for the soil moisture content. Similarly, potential evapotranspiration is associated with a correction factor K_{ep} and G_0 is the depth of initial groundwater storage. The maximum groundwater storage parameter (G_{max}) is dependent on groundwater depth and K_{run} is an exponent for reflecting the effect of small rainfall intensity on surface runoff. P_{max} is also a modeling time-dependent threshold for rainfall intensity.

Since snow melt and accumulation do not occur in the Werii watershed, the temperature data were not taken as an input for the modeling process. Hence, the global model parameters of the base temperature (TO) and degree day coefficient (K_{snow}), as well as the rainfall degree day coefficient (K_{rain}), were set to a negative value (-1) so that the model ignored them during simulation.

Split-sample techniques were used for the calibration and validation processes. Hence, data recorded within a similar timescale for all the meteorological parameters and spatial data

Table 3

Parameter values of the WetSpa model with WetSpa simulated watershed threshold values and corresponding measurement units.

Parameters with common threshold values	Unit	Value/estimated
Stream network delineating threshold	Cells	10
Sub catchments determining threshold value	Cells	1000
Upstream drained area by a particular cell	Km^2	>0.1
Sub catchments	Total	96
Average sub catchment area	Km^2	18.7
Average hydraulic radius at upland cells	Meter	0.005
Average hydraulic radius at outlets	Meter	1.5
Time of concentration	Hour	58
Mean travel time for entire watershed	Hour	23
Manning's coefficient for lowest order	$\text{m}^{-1/3} \text{ s}$	0.055
Manning's coefficient for highest order	$\text{m}^{-1/3} \text{ s}$	0.025
Impervious area within an urban cell	%	30

Table 4

Main calibration parameters of the WetSpa model for the Werii watershed.

Global model Parameters	Description	Unit
K_i	Interflow scaling parameter	—
K_g	Groundwater recession coefficient	—
K_{ss}	Relative soil moisture	—
K_{ep}	Correction coefficient for potential evapotranspiration	—
G_0	Initial groundwater storage	mm
G_{max}	Maximum groundwater storage	mm
TO	Base temperature for estimating snow melt	°C
K_{snow}	Degree day coefficient for calculating snow melt	mm/mm/°C/d
K_{rain}	Rainfall degree day coefficient	mm/mm/°C/d
K_{run}	Surface runoff coefficient	—
P_{max}	Threshold rainfall intensity	mm/d

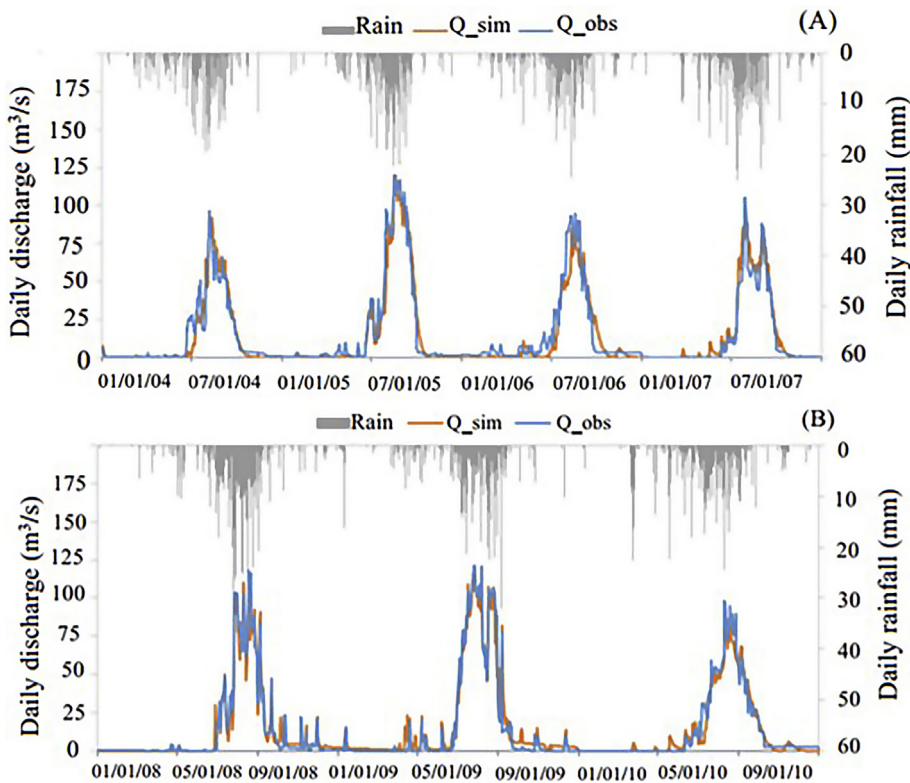


Fig. 4. Werii watershed simulation (Q_{sim} = simulated discharge, Q_{obs} = observed discharge) (A), Model calibration results from 1 January 2004 to 31 December 2007 and (B), Validation period from 1 January 2008 to 31 December 2010.

derived from the base maps of topography, land use, and soil texture were used for calibration as well as validation in the modeling process.

Model calibration was undertaken using the graphical fit between simulated and observed discharges (Fig. 4A) and model performance evaluating criteria (Table 5). The WetSpa model validation result is also given in Fig. 4B. Both the statistical and graphical comparison of the observed and simulated discharge confirmed that the WetSpa had captured the observed discharges well. These calibration results were obtained with a repetitive trial and error method to fine-tune the global parameters within their range. The best fit values created between observed and simulated discharges for the Werii watershed during the calibration process are shown in Table 6. The statistical model performance evaluation results for both calibration and validation processes are also indicated in Table 5. Model bias (MB), model confidence (R^2) and Nash-Sutcliffe efficiency (NSE) were used as the WetSpa model performance evaluating measures.

The daily discharge frequency curve for the observed and simulated period is depicted in Fig. 5. This frequency curve shows that the observed and simulated discharges have a consistent pattern in the simulation period and there was good agreement between the observed and simulated values.

Table 5

Model performance evaluation results of WetSpa model for the calibration and verification on a daily basis.

Run	Model bias	Coefficient of determination	Nash-Sutcliffe efficiency
Calibration	0.03	0.87	0.77
Validation	-0.07	0.92	0.79
Optimum	0	1	1

Therefore, the analysis showed that it would be reasonable to use the model to simulate future water resources change in the watershed. This was done using an input data simulated using the SDSM model for the future (2015–2050) time horizon.

Water resources of the base period (2008–2010)

The actual evapotranspiration, groundwater recharge, surface runoff, interflow and soil moisture content at the outlet were simulated for the base period in grid format while the rest of the water balance components were provided in text format. The simulated spatial grid files were further interpreted in arc GIS for further analysis of the spatial variations for the separate portions of the watershed. More detailed analysis of the spatial groundwater distributions of the watershed in seasonal and annual basis can be found in [Gebremeskel and Kebede \(2017\)](#).

Table 6

WetSpa model parameters and calibration result for the Werii watershed.

Parameter	Value range	Calibration result
K_i	0–12	1.0004
K_g	0–0.06	0.04225
K_{ss}	0–2	0.5871
K_{ep}	0–2	0.46525
G_O	0–100	14.500
G_{max}	0–3000	7.500
T_O	0–1	-1.00
K_{snow}	0–10	-1.00
K_{rain}	0–0.05	-1.00
K_{run}	0–5	4.500
P_{max}	0–500	230.00

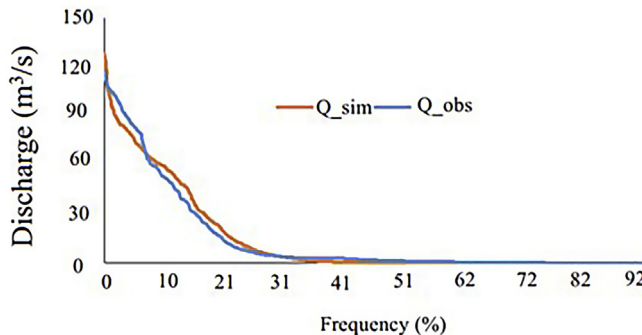


Fig. 5. Observed and simulated daily discharge frequency curves for Werii watershed.

The average annual water balance components for each calibration and validation period were simulated and are presented in Table 7. The mean and maximum values of the water balance components are also presented in Table 7. Similarly, runoff, actual evapotranspiration, groundwater recharge, interflow and soil moisture were simulated as spatial distribution grid maps during the simulation process. The analysis in Table 7 shows that the average annual actual evapotranspiration (651.64 mm), surface runoff (42.62 mm) and recharge (37.84 mm) were obtained as 89%, 5.8% and 5% of the annual average rainfall (732.10 mm) respectively, and this result was in agreement with the findings of Beyene et al. (2011) and Tesfamichael et al. (2013) in the Giba catchment of Ethiopia.

The baseflow was obtained as the sum of the interflow and groundwater flow simulated from the model. Therefore, the analysis showed that the baseflow (223.95 mm) was 7% (16.13 mm) of the interflow and 92.8% (207.83 mm) of the groundwater flow. The runoff (266.57 mm) was 16% (42.62 mm) of the surface runoff and 84% (223.95 mm) of the baseflow which were similar trends to the findings of Nyenje and Batelaan (2009). Due to the uni-modal rainfall distribution in Werii watershed, the simulated average runoff was mainly contributed by baseflow especially in the dry season.

SDSM model calibration and validation

The SDSM model was calibrated for each of the meteorological stations considered in this study. Figs. 6–8 show the rainfall, maximum and minimum temperature calibration results of the SDSM model for each station, respectively. For most of the stations, the MAE approached its optimum value after the repetitive trial and error calibration technique. As a result, the MAE and STD values revealed that the SDSM model was well calibrated for this watershed. After model calibration, the validation of the SDSM model was undertaken to downscale the future changes in climate from

the REMO dataset based on the A1B and B1 SRES emission scenarios.

The calibration of REMO datasets with the locally observed data of each meteorological station was well captured by the SDSM model based on the observed model evaluations indices of RAE and SD. As indicated in Fig. 6, the Adigrat and Abyadi stations had relatively better calibration results than the Hawzen and Adwa stations. Similarly, the calibration of maximum and minimum temperatures (Figs. 7 and 8, respectively) was reliable and acceptable. Generally, a temperature is easily calibrated compared to precipitation. This could be due to the conditional climate characteristics associated with rainfall events in the watershed.

Effects of climate change on water resources

Projected change in rainfall and temperature

The SDSM model calibration results of the rainfall, a maximum and minimum temperature for Werii watershed are given in Figs. 6–8, respectively. Table 8 shows the predicted rainfall, minimum and maximum temperatures for the period from 2015 to 2050. The analysis showed that there was an increment in rainfall and temperature in the Werii watershed. More details of the climate projection analysis for rainfall and temperatures for the watershed can be found in Haile and Kasa (2015). Rainfall in the watershed is likely to show an increment over the next 35 yr horizon of 24% under the A1B scenario and 25.3% under the B1 scenario. This result was consistent with the findings of the Intergovernmental Panel on Climate Change (2013), Kebede et al. (2013), Kim et al. (2008) and Nyenje and Batelaan (2009). The current annual average rainfall (732.10 mm) increase to 912 mm due to increments after 35 yr. Similarly, the minimum temperature was projected to increment by 0.17 °C under the A1B scenario and by 0.165 °C under the B1 scenario, while the maximum temperature was expected to increase by 0.09 °C under the A1B scenario and by 0.07 °C under the B1 scenario. The change in minimum temperature was faster and greater than for the maximum temperature. Such change is common globally (Paeth et al., 2005; Gebrehiwot and van der Veen, 2013) which indicates warming nights have occurred in recent times.

Projected changes in water resources

The SDSM model results for the future period (2015–2050) were based on the climate parameter data of rainfall and PET (as a result of minimum and maximum temperatures) as inputs for the calibrated and validated WetSpa model. As a result, the future water balance components were estimated and the climate change effects were assessed further. The water resources change for the future period (2015–2050) under A1B and B1 SRES were predicted as

Table 7

Comparison of water balance components based on observed, calibration and validation results in the Werii watershed.

Water balance components	Measured data annual average (2004–2010) (mm)	Calibration period (2004–2007)			Validation period (2008–2010)		
		Annual average (mm)	Mean	Maximum	Annual average (mm)	Mean	Maximum
Rainfall	735.23	740.54	2.39	38.10	732.10	2.04	36.10
Interception		86.00	0.23	2.40	88.48	0.24	2.22
Surface runoff		46.40	0.10	2.90	42.62	0.07	2.63
Infiltration		605.56	1.94	32.90	600.58	1.64	32.50
Evapotranspiration	1,685.88	653.08	1.33	5.64	651.64	1.31	4.82
Percolation		291.11	0.88	17.06	282.24	0.77	16.90
Interflow		17.10	0.07	1.00	16.13	0.04	0.89
Groundwater flow		210.50	0.60	5.20	207.83	0.57	4.66
Baseflow		229.57	0.88	2.30	223.95	0.61	5.55
Total runoff	248.45	260.55	0.71	7.55	266.57	0.68	7.17
Soil moisture storage		−74.09	—	—	−92.10	—	—
Groundwater storage		−99.00	—	—	−94.01	—	—

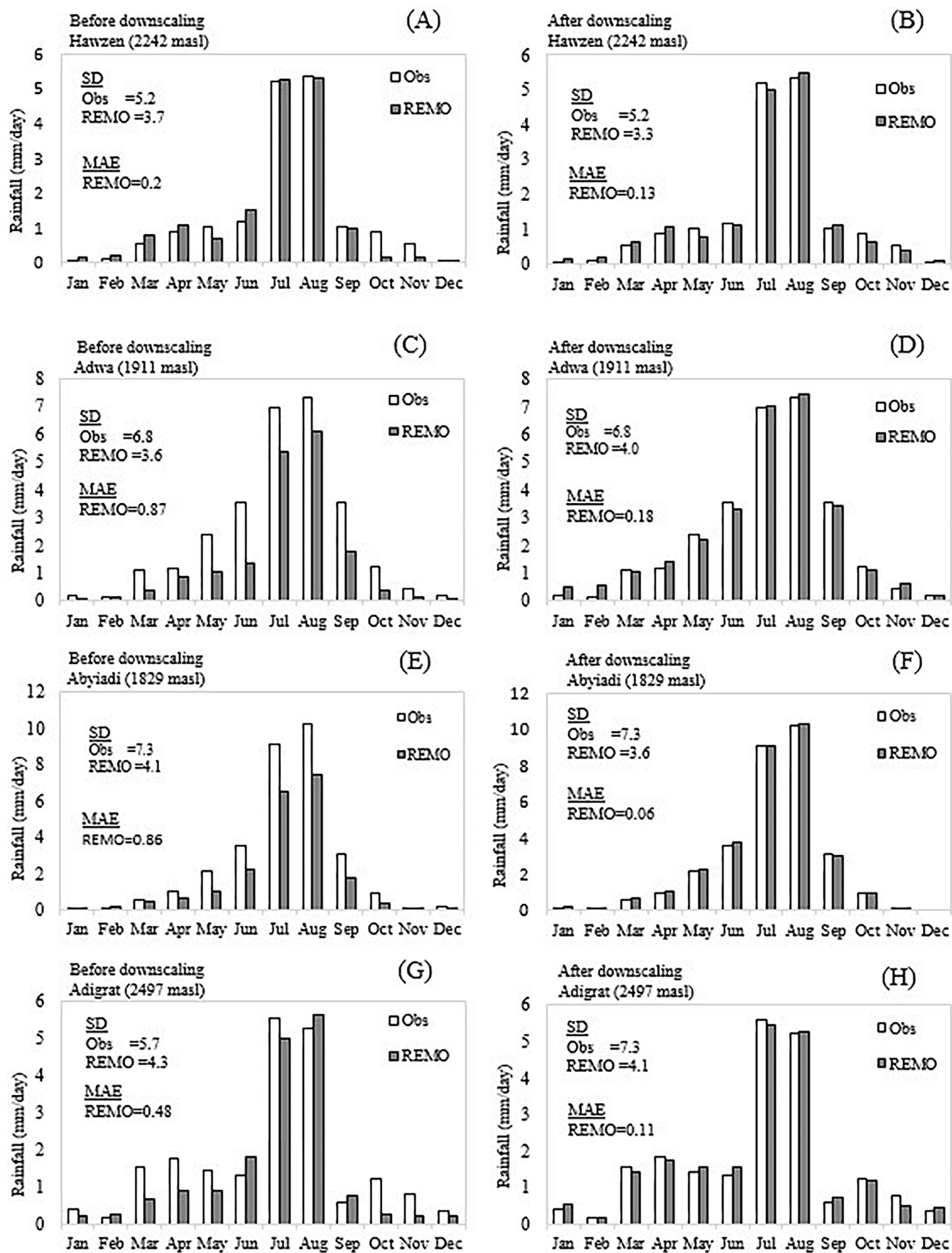


Fig. 6. Before and after downscaling of rainfall at each meteorological station (Observed = Obs and REMO data). Note: masl = meters above sea level, MAE = mean absolute error.

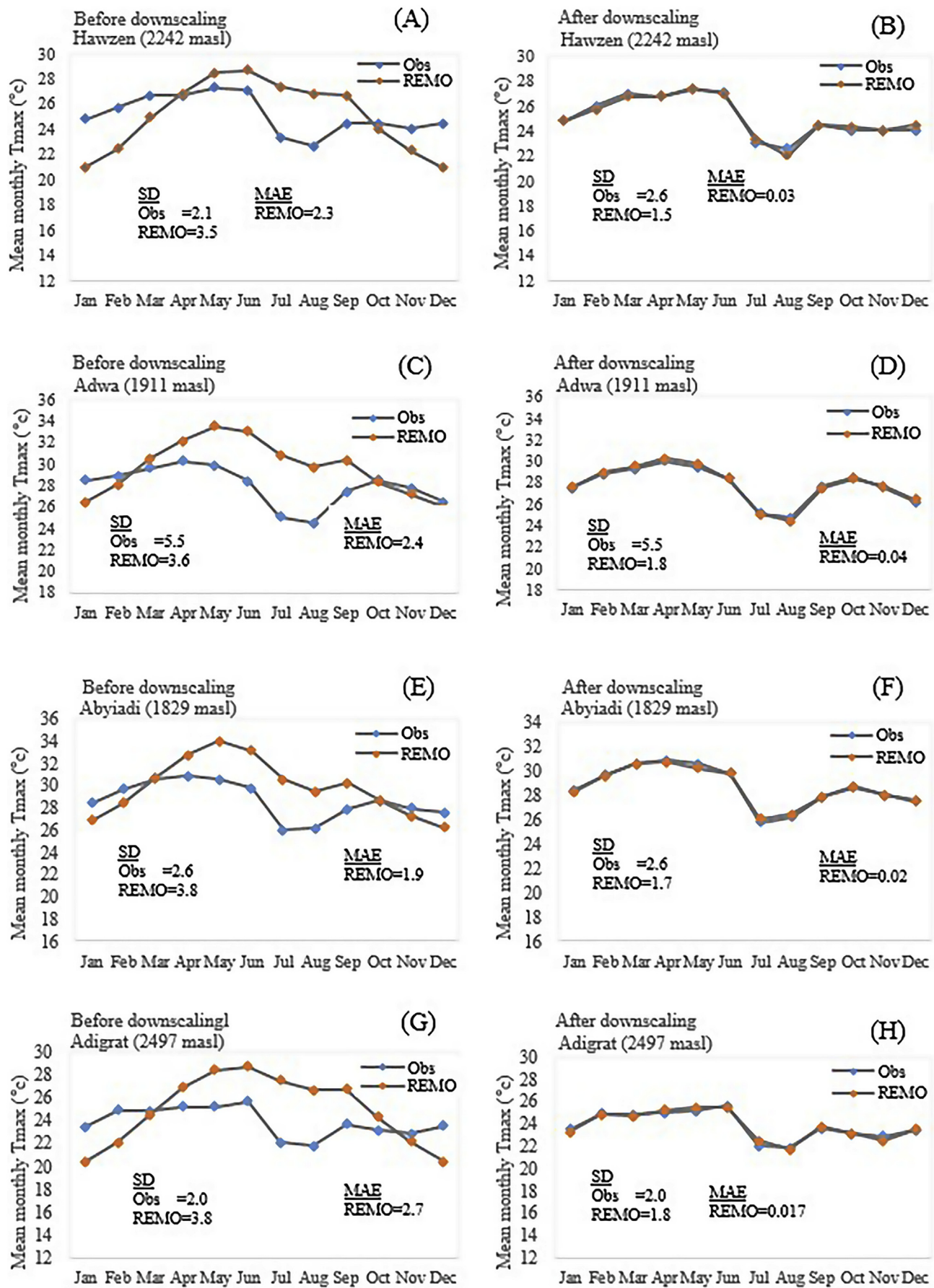


Fig. 7. Before and after downscaling of each meteorological station (Observed and REMO maximum temperature data). Note: masl = meters above sea level, MAE = mean absolute error.

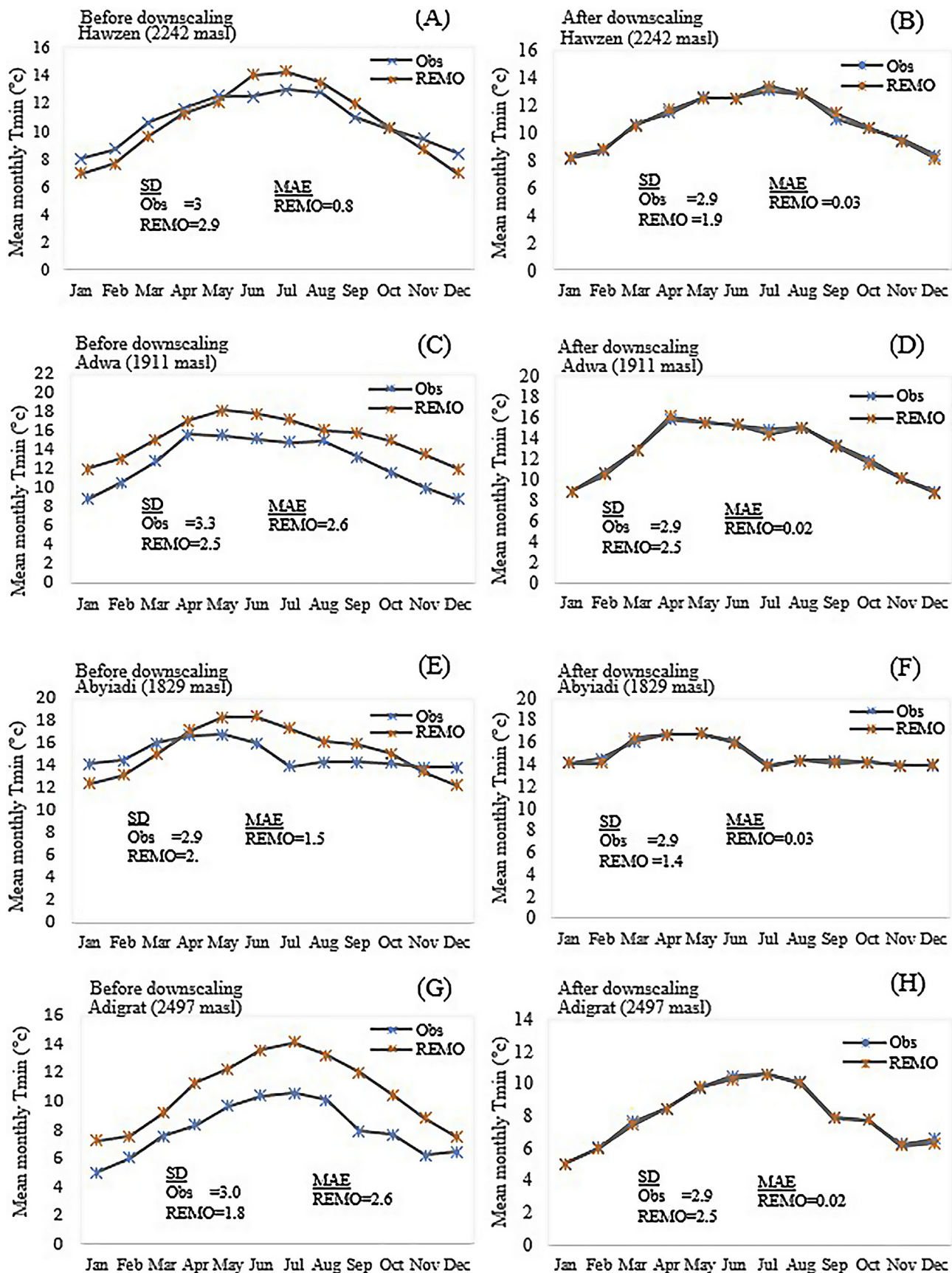


Fig. 8. Before and after downscaling of each meteorological station (Observed and REMO minimum temperature data). Note: masl = meters above sea level, MAE = mean absolute error.

Table 8

Simulated future periods (2015–2050) climate projections based on A1B and B1 SRES emission scenario in the Werii watershed.

Meteorological parameter (Average values)	SRES emission scenarios		
	A1B	B1	Combined average
Rainfall	24%	25.3%	24.65%
Minimum temperature	0.170 °C	0.165 °C	0.168 °C
Maximum temperature	0.09 °C	0.07 °C	0.08 °C

Table 9

Annual water balance percentage change compared to the base period (2008–2010).

Water balance component	Base period (2008–2010)	Future A1B scenario (2015–2050)		Future B1 scenario (2015–2050)	
		Annual average (mm)	Change (%)	Annual average (mm)	Change (%)
Rainfall	732.10	907.80	24.0	917.32	25.3
Evapotranspiration	651.64	749.50	15.0	767.02	18.0
Recharge	37.84	39.73	5.0	38.54	2.0
Surface runoff	42.62	37.02	−13.0	36.64	−14.0
Baseflow	223.95	255.30	14.0	241.97	8.0

depicted in Table 9. Therefore, a list of the main water balance components was provided and their future changes were analyzed based on the indicative SRES A1B and B1 emission scenarios. As a result, the rainfall, evapotranspiration, recharge, and baseflow showed an increment while runoff showed a decrement. The actual evapotranspiration was likely to increase by 15% under A1B and by 18% under B1, which showed similar projections to rainfall. This result showed a trend consistent with the upper Blue Nile River over the same time horizon which had a predicted 16% increase on average (Kim and Kaluarachchi, 2009). The results of the current study indicate that the future groundwater recharge is expected to increase by 5% and 2% from the base period under the A1B and B1 scenarios, respectively. This will also occur as a result of the increment in rainfall for this time horizon. In general, the groundwater recharge simulated for both scenarios would increase and be maximized under the A1B scenario. This result was also in agreement with the findings of Nyenje and Batelaan (2009) and Obubie et al. (2008).

Moreover, the baseflow produced as a result of interflow and groundwater flow was likely to show an increasing trend by 14% under the A1B scenario and by 8% under the B1 scenario. The baseflow is more sensitive in the A1B scenario as it is higher by 6% than in the B1 scenario. Unlike the baseflow, the surface runoff would show a decreasing trend for both emission scenarios. As a result, the surface runoff was expected to decrease by 13% under A1B and by 14% under B1. The likely reason for this decrement in runoff is the implementation of exclosures and soil and water conservation activities in the Werii watershed. Haregeweyn et al. (2015) indicated that integrated watershed management works in the watershed have reduced the overall land degradation in the past two decades. As a result, the rainfall that would have been runoff has either percolated to the groundwater table or evaporated back into the atmosphere.

It can be concluded that the future hydrological water resources changes would be likely to occur for the emission scenarios considered in this study. The rainfall, actual evapotranspiration, and baseflow would likely increase. The watershed dwellers are expected to use the increased water resources for irrigation and consumptive purposes.

Conclusion

Available water resources in the base period and future changes were quantified for each of the water balance components through the integrated use of the climate and hydrological models. The

future water resources by the end of 2050 were investigated after downscaling future rainfall and temperature from REMO dataset outputs through using the SDSM model. Due to the effect of climate change, the rainfall is likely to increase with a combined average of 24.65% for both the A1B and B1 scenarios. In the same manner, the change in minimum temperature is 0.168 °C which is faster and greater than for the maximum temperature (0.08 °C), which indicates warming nights are occurring over time. The downscaled future rainfall and PET were used as inputs to the WetSpa model to simulate future water resources. It can be concluded that the future hydrological water resources are likely to increase under the emission scenarios A1B and B1. The groundwater recharge, actual evapotranspiration, and baseflow would increase while runoff would reduce. Accordingly, due to climate change, the Werii watershed will experience decreased surface runoff due to the watershed protection measures in the watershed. The Werii watershed should keep watershed management approaches in terms of increased vegetation cover, soil and water conservation interventions. This could accommodate the water resource increments in the Werii watershed. All this would be used to increase the groundwater storing capacity, especially in rainy seasons. Therefore, optimal allocation of the groundwater resources is useful for irrigation and consumptive uses.

This study used an integrated use of climatic and hydrological models to predict the effects of climatic factors on the hydrology of the watershed. These findings provide a basis for further analysis and understanding of the downscaled climate data to be used for a hydrological model for simulating future hydrological parameters. A detail study of seasonal water resources and of the spatial and temporal variations of the climatic and hydrological factors is useful to effectively determine the longer dry and short wet periods that may occur in the Werii watershed.

Conflict of interest

The authors declare no conflict of interest.

Acknowledgments

The authors would like to acknowledge the Ethiopian National Meteorological Service Agency for the provision of the meteorological data used for this study. Daily discharge data were also obtained from the Ethiopian Ministry of Water Resources, Irrigation and Energy. This research was financed by the Tigray Agricultural Research Institute and ILRI, LIVES Project, Ethiopia.

References

Alcamo, J., Döll, P., Kaspar, F., Siebert, S., 1997. Global Change and Global Scenarios of Water Use and Availability: an Application of Water GAP1.0. Center for Environmental Systems Research, University of Kassel, Germany.

Allen, R.G., Raes, D., Smith, M., 1998. Crop Evapotranspiration (Guidelines for Computing Crop Water Requirements) FAO Irrigation and Drainage Paper No. 56. FAO: Water Resources Development and Management Service, Rome, Italy.

Araya, A., Stroosnijder, L., 2011. Assessing drought risk and irrigation need in Northern Ethiopia. *Agric. For. Meteorol.* 151, 425–436.

Awulachew, S.B., Yilma, A.D., Lousegd, M., Loiskandl, W., Ayana, M., Alamirew, T., 2007. Water Resources and Irrigation Development in Ethiopia. International Water Management Institute, Working Paper 123, Colombo, Sri Lanka, p. 78.

Beyene, Y.A., Batelaan, O., Goitom, H., 2011. Spatial and Temporal Simulation of Groundwater Recharge for Geba Catchment, Northern Ethiopia Using WetSpa. MSc. Thesis. Universiteit Gent, Vrije Universiteit Brussels, Belgium.

Brooks, R.H., Corey, A.T., 1966. Properties of porous media affecting fluid flow. *J. Irr. Drain. Div. ASCE* 92, 61–90.

Food and Agriculture Organization of the United Nations, 1998. Land and Water Digital Media Series – the Soil and Terrain Database for Northeastern Africa. FAO, Land and Water Digital Media Series no. 2, Rome, Italy.

Gebrehiwot, T., van der Veen, A., 2013. Assessing the evidence of climate variability in the northern part of Ethiopia. *J. Dev. Agric. Econ.* 5, 104–119.

Gebremeskel, G., Kebede, A., 2017. Spatial estimation of long-term seasonal and annual groundwater resources: application of WetSpa model in the Werri watershed of the Tekeze River Basin, Ethiopia. *Phys. Geogr.* 38, 338–359.

Gupta, H.V., Sorooshian, S., Yapo, P.O., 1999. Status of automatic calibration for hydrologic models: comparison with multilevel expert calibration. *J. Hydrol. Eng.* 4, 135–143.

Hadgu, G., Kindie, T., Girma, M., Belay, K., 2013. Trend and variability of rainfall in Tigray, Northern Ethiopia: analysis of meteorological data and farmers' perception. *Acad. J. Agric. Res.* 1, 88–100.

Hadgu, G., Kindie, T., Girma, M., 2015. Analysis of climate change in Northern Ethiopia: implications for agricultural production. *Theor. Appl. Climatol.* 117, 733–747.

Haile, G.G., Kassa, A.K., 2015. Investigation of precipitation and temperature change projections in Werri watershed, Tekeze river basin, Ethiopia; application of climate downscaling model. *J. Earth Sci. Clim. Change* 6, 300. <https://doi.org/10.4172/2157-7617.1000300>.

Haregeweyn, N., Tsunekawa, A., Nyssen, J., Poesen, J., Tsubo, M., Meshera, D.T., Schutt, B., Adgo, E., Tegegne, F., 2015. Soil erosion and conservation in Ethiopia: a review. *Prog. Phys. Geogr.* 1–25.

Inter-Governmental Panel on Climate Change, 2013. Climate Change 2013: the Physical Science Basis. Contribution of Working Group I to the Fifth Assessment Report of the Inter-governmental Panel on Climate Change. Cambridge University Press, Cambridge, UK.

Jacob, D., 2001. A note to the simulation of the annual and inter-annual variability of the water budget over the Baltic Sea drainage basin. *Meteorol. Atmos. Phys.* 77, 61–73.

Kebede, A., Diekkrüger, B., Moges, S.A., 2013. An assessment of temperature and precipitation change projections using a regional and a global climate model for the Baro-Akobo Basin, Nile Basin, Ethiopia. *J. Earth Sci. Clim. Change* 4, 133. <https://doi.org/10.4172/2157-7617.1000133>.

Kim, U., Kaluarachchi, J.J., 2009. Climate change impacts on water resources in the upper Blue Nile river basin, Ethiopia. *J. Am. Water Resour. Assoc.* 45, 1361–1378.

Kim, U., Jagath, J.K., Vladimir, U.S., 2008. Generation of monthly precipitation under climate change for the upper Blue Nile river basin, Ethiopia. *J. Am. Water Resour. Assoc.* 44, 1232–1247.

Kumar, C.P., 2012. Climate change and its impact on groundwater resources. *Int. J. Eng. Sci.* 1, 43–60.

Legates, D.R., McCabe, G.J., 1999. Evaluating the use of "goodness-of-fit" measures in hydrologic and hydroclimatic model validation. *Water Resour. Res.* 35, 233–241.

Liu, Y.B., De Smedt, F., 2004. WetSpa Extension, a GIS-based Hydrologic Model for Flood Prediction and Watershed Management, Documentation and User Manual. Department of Hydrology and Hydraulic Engineering, Vrije Universiteit Brussel, Brussels, Belgium.

Makombe, G., Kelemework, D., Areo, D., 2007. A comparative analysis of rainfed and irrigated agricultural production in Ethiopia. *Irrigat. Drain. Syst.* 21, 35–44.

Melesse, A.M., 2011. Nile River Basin Hydrology, Climate and Water Use, Department of Earth and Environment, Florida International University, Modesto a. Maidique Campus, Miami, FL, USA.

Moriasi, D.N., Arnold, J.G., Van Liew, M.W., Bingner, R.L., Harmel, R.D., Veith, T.L., 2007. Model evaluation guidelines for systematic quantification of accuracy in watershed simulations. *Am. Soc. Agric. Biol. Eng.* 50, 885–900.

Moss, R.H., Edmonds, J.A., Hibbard, K.A., Manning, M.R., Rose, S.K., van Vuuren, D.P., Carter, T.R., Emori, S., et al., 2010. The next generation of scenarios for climate change research and assessment. *Nature* 463, 747–756.

Nash, J.E., Sutcliffe, J.V., 1970. River flow forecasting through conceptual model. *J. Hydrol.* 10, 282–290.

Nyenje, P.M., Batelaan, O., 2009. Estimating the effects of climate change on groundwater recharge and base flow in the upper Ssezibwa catchment, Uganda. *Hydrolog. Sci. J.* 54, 713–725.

Obuobie, E., Diekkrüger, B., Reichert, B., 2008. Estimation of Groundwater Recharge in the Context of Future Climate Change in the White Volta River Basin, West Africa. PhD thesis. Faculty of Mathematics and Natural Sciences, University of Bonn, Germany.

Paeth, H., Kaib, O., Ralf, P., Daniela, J., 2005. Regional dynamical downscaling over West Africa: model evaluation and comparison of wet and dry years. *Meteorol. Z.* 14, 349–367.

Raghunath, H.M., 2006. Hydrology Principles, Analysis and Design, Revised Ed. New Age International, New Delhi, India.

Santhi, C., Arnold, J.G., Williams, J.R., Dugas, W.A., Srinivasan, R., Hauck, L.M., 2001. Validation of the SWAT model on a large river basin with point and nonpoint sources. *J. Am. Water Resour. Assoc.* 37, 1169–1188.

Soliman, E.S., Sayed, M.A., Jeuland, M., 2009. Impact assessment of future climate change for the Blue Nile basin using a RCM nested in a GCM. *Nile Basin Water Eng. Sci. Mag.* 2, 15–30.

Tesfamichael, G., De Smedt, F., Walraevens, K., Gebresilassie, S., Hussien, A., Gebrehiwot, K., 2013. Application of a spatially distributed water balance model for assessing surface water and groundwater resources in the Geba basin, Tigray, Ethiopia. *J. Hydrol.* 499, 110–123.

Wang, Z.M., Batelaan, O., De Smedt, F., 1997. A distributed model for water and energy transfer between soil, plants and atmosphere (WetSpa). *Phys. Chem. Earth* 21, 189–193.

Wilby, R.L., Charles, S.P., Zorita, E., Timbal, B., Whetton, P., Mearns, L.O., 2004. Guidelines for Use of Climate Scenarios Developed from Statistical Downscaling Methods. Supporting material of the Intergovernmental Panel on Climate Change, available from the DDC of IPCC TGCIA, London, UK, p. 27.

Wilby, R.L., Dawson, C.W., 2007. SDSM 4.2-A Decision Support Tool for the Assessment of Regional Climate Change Impacts. User manual, London, UK, p. 94.

Willmott, C.J., Kenji, M., 2005. Advantages of the mean absolute error (MAE) over the root mean square error (RMSE) in assessing average model performance. *Clim. Res.* 30, 79–82.

Yazew, E., 2005. Development and Management of Irrigated Lands in Tigray, Ethiopia. PhD. thesis. UNESCO-IHE Institute for Water Education, Delft, the Netherlands.